MATHEMATICAL SCIENCES

A GEOMETRIC MODEL OF THE TWISTED OUTER BIPOLAR SHELL OF A VORTEX KERN

Milyute E.
Department of Mathematical Computer Science, Vilnius University and IRG"LITAVEM-3"
Milyus A.
IRG "LITAVEM-3"
Vilnius, Lithuania
https://doi.org/10.5281/zenodo.21706149

Abstract

A geometric model of a twisted bipolar outer shell surrounding a vortex kern is proposed for describing a smooth bipolar microvortex structure with continuous helical filaments. The bipolar coordinate system is derived from a complex Möbius (fractional linear) transformation that maps two distinguished poles to the origin and infinity, followed by the application of the complex logarithm. An analytical representation of the coordinate mapping is obtained, and the circular nature of the coordinate curves, the orthogonality of the coordinate families, and the conformal form of the metric are established. To describe the internal rotation of the shell, a smooth twist function, $\Omega(\tau)$, is introduced, transforming the angular coordinate according to $\sigma' = \sigma + \Omega(\tau)$. It is shown that this transformation converts the untwisted bipolar coordinate network into a system of continuous helical filaments while preserving the bipolar topology, the number of poles, and the local smoothness of the mapping. The Jacobian of the transformation, the metric tensor, and the conditions for orientation preservation are investigated. A numerical study employing the localized twist function $\Omega(\tau) = k\tanh(\lambda\tau)$ demonstrates that increasing the twist parameter leads to an increase in filament length and curvature and to the formation of a pronounced helical structure surrounding the inner vortex kern. The proposed construction provides a geometric framework for further investigations of the stability, helicity, and topological invariants of closed vortex shells.

Keywords: vortex kern; bipolar coordinates; twisted bipolar shell; vortex filaments; conformal mapping; stereographic projection; Möbius transformation; logarithmic mapping; differential geometry; geometric hydrodynamics; vortex topology; helicity; microvortex; vortex shell; numerical simulation

1. Introduction. The study of vortex structures is one of the fundamental research directions in modern hydrodynamics, mathematical physics, and geometric mechanics. Vortices arise in a wide range of natural and engineering processes, including turbulent flows, atmospheric and oceanic circulation, plasma physics, biomechanics, and aerodynamics. Despite significant advances in computational modeling, the geometric structure of individual vortices and the mechanisms governing the formation of their internal shells remain subjects of active investigation.

The classical theory of vortex motion originates from the work of Hermann von Helmholtz [1], who formulated the fundamental laws governing the evolution of vortex tubes in an ideal fluid. These ideas were subsequently developed by William Thomson, 1st Baron Kelvin, who demonstrated that the circulation around a material contour is conserved over time under the assumptions of ideal hydrodynamics. Kelvin's circulation theorem became one of the cornerstones of the geometric interpretation of vortex flows, establishing a fundamental relationship between fluid motion and the preservation of the topology of vortex lines.

During the twentieth century, vortex theory underwent substantial development through studies of vortex filaments and vortex tubes. It was established that vorticity is naturally transported by the fluid flow and that vortex filaments possess a high degree of geometric coherence and structural stability. Significant contributions to the understanding of the local geometry of vortices were made by Luigi da Rios, Horace Lamb, Philip G. Saffman, Harry Bateman, and many other researchers [3-8, 23, 32-35, 38-42], who investigated the evolution of thin vortex filaments and their relationship to the governing equations of hydrodynamics.

Simultaneously, methods of differential geometry underwent rapid development [9-16, 24, 26-27, 36-37]. The introduction of the Frenet–Serret frame made it possible to describe vortex lines as space curves characterized by curvature and torsion. It was subsequently shown that the local geometry of a vortex filament is directly related to its dynamical evolution [40-42]. Of particular importance is the Hiroshi Hasimoto transformation, which converts the localized induction equation of a vortex filament into the nonlinear Erwin Schrödinger equation [31]. This remarkable result established, for the first time, a profound connection between the geometry of space curves and nonlinear wave phenomena.

Considerable attention has also been devoted to the study of topological invariants of vortex structures. The work of Henry Keith Moffatt [6-7] demonstrated that helicity is an integral measure of the mutual linkage and knottedness of vortex lines and may be regarded as a topological invariant of the flow. The theory was later extended through the introduction of Heinz Hopf invariants, which provide a rigorous algebraic-topological framework for describing complex spatial entanglements of vortex filaments [28-30].

In parallel, methods of conformal geometry and complex analysis were actively developed [17-20]. The stereographic projection, Möbius transformations, and complex coordinate systems became powerful tools for the investigation of surfaces of constant curvature [38, 40]. Conformal mappings preserve the angles between intersecting curves and are therefore particularly well suited for the analysis of vortex flows, whose local structure is primarily determined by the angular properties of rotational motion.

A special role is played by the theory of bipolar coordinates [21-25]. This coordinate system arises naturally in the presence of two fixed poles and is widely used in electrostatics, potential theory, and conformal mapping. Bipolar coordinates are defined by the transformation

$$x = \frac{a\sin\sigma}{\cosh\tau - \cos\sigma}, \qquad y = \frac{a\sinh\tau}{\cosh\tau - \cos\sigma}, \quad (1)$$

where the parameter a determines the distance between the two foci of the coordinate system. Owing to the conformality of this mapping, the coordinate curves form two orthogonal families of circles, making bipolar coordinates a convenient tool for describing bipolar geometric objects.

In classical applications, bipolar coordinates are used primarily for solving elliptic equations and problems of potential theory [24]. However, their application to the description of the internal structure of vortex shells has remained virtually unexplored. Meanwhile, the presence of two singular points naturally corresponds to the model of a vortex kern having two ends connected by a common internal structure.

In the present work, a geometric model is considered in which the microvortex shell is described not as a collection of independent vortex surfaces but as a single smooth two-dimensional manifold with two poles. The principal element of the model is an internal twist of the coordinate system, described by the smooth function

$$\sigma' = \sigma + \Omega(\tau), \quad (2)$$

where the function $\Omega(\tau)$ specifies the distribution of the internal rotation angle along the axis of the vortex kern. This formulation makes it possible to describe the continuous formation of helical filaments without violating the smoothness of the surface.

It should be emphasized that the proposed model is a geometric construction. It is not derived directly from the Navier–Stokes equations and is not intended to describe the complete hydrodynamic process. Its purpose is to establish a mathematically consistent geometry of a vortex shell that can subsequently serve as a foundation for further investigations of its dynamics, stability, helicity, and topological invariants.

The primary objective of the present work is to develop an analytical model of a twisted bipolar shell, to investigate its metric properties, to derive the conditions for the smoothness of the mapping, and to analyze the geometric characteristics of the resulting vortex filaments. Particular attention is devoted to the manner in which the local coordinate twist transforms the orthogonal bipolar coordinate network into a system of continuous helical lines connecting both ends of the inner vortex kern and forming a single closed vortex shell.

2. Rigorous Derivation of Bipolar Coordinates from a Complex Mapping.

Consider the complex plane with coordinate

$$z = x + iy \quad (3)$$

and fix two distinguished points

$$F_+ = ia, F_- = -ia, a > 0. \quad (4)$$

In Cartesian coordinates, these points are given by

$$F_+ = (0, a), F_- = (0, -a). \quad (5)$$

To construct the bipolar coordinate system, we introduce the Möbius (fractional linear) transformation

$$\zeta = (z - ia)/(z + ia). \quad (6)$$

This transformation maps the upper pole $z = ia$ to the origin of the complex plane:

$$z = ia \implies \zeta = 0,$$

and the lower pole $z = -ia$ to the point at infinity:

$$z = -ia \implies \zeta = \infty .$$

Since Möbius transformations are conformal at every point where their derivative is nonzero, this mapping preserves the angles between smooth curves everywhere except at the poles. Let the new complex variable be represented in exponential form

$$\zeta = e^{\omega}, \omega = \tau + i\sigma, \quad (7)$$

where $\tau \in \mathbb{R}$, and the angular coordinate σ is defined modulo 2π:

$$\sigma \sim \sigma + 2\pi.$$

Thus,

$$(z - ia)/(z + ia) = e^{\tau + i\sigma} . \quad (8)$$

Taking the complex logarithm of both sides yields the direct definition of the bipolar coordinate:

$$\tau + i\sigma = \log((z - ia)/(z + ia)), \quad (9)$$

whose real part gives

$$\tau = \ln|(z - ia)/(z + ia)| , \quad (10)$$

and whose imaginary part is

$$\sigma = arg(z - ia) - arg(z + ia) \ (\mathrm{mod}\ 2\pi) . \quad (11)$$

Hence, the coordinate τ represents the logarithm of the ratio of the distances from the point z to the two poles, whereas the coordinate σ is the oriented difference between the angles subtended by these poles as viewed from the point z. If the distances from the point z to the poles are denoted by

$$\begin{aligned} r_+ &= |z - ia| = \sqrt{x^2 + (y - a)^2}, \\ r_- &= |z + ia| = \sqrt{x^2 + (y + a)^2}, \end{aligned} \quad (12)$$

then

$$e^{\tau} = r_+/r_- . \quad (13)$$

The sign τ indicates which pole the point is closer to. For $\tau < 0$, one has $r_+ < r_-$, meaning that the point is closer to F_+ , whereas for $\tau > 0$, it is closer to F_-. The line $\tau = 0$ satisfies the condition $r_+ = r_-$ and therefore coincides with the perpendicular bisector of the segment F_+F_- , that is, with the axis $y = 0$.

We now derive the inverse transformation. From the relation

$$e^{\omega} = (z - ia)/(z + ia) \quad (14)$$

it follows that

$$z - e^{\omega} z = ia + iae^{\omega} , z = ia((1 + e^{\omega})/(1 - e^{\omega})) \quad (15)$$

Using the indenity

$$\coth\frac{\omega}{2} = \frac{e^{\omega}+1}{e^{\omega}-1} \quad (16)$$

we obtain

$$(1 + e^{\omega})/(1 - e^{\omega}) = -\coth(\omega/2) . \quad (17)$$

Therefore,

$$z = -ia\coth(\omega/2) \quad (18)$$

The choice of the initial ratio involving the poles determines possible changes in the signs and orientation of the coordinates. To obtain the form adopted below, with the poles located on the vertical axis, it is convenient to write the mapping equivalently as

$$z = (a\sin\sigma + ia\sinh\tau)/(\cosh\tau - \cos\sigma) \quad (19)$$

We now derive this formula directly. For the complex argument $\omega = \tau + i\sigma$ we have

$$\coth\frac{w}{2} = \frac{\sinh\tau - i\sin\sigma}{\cosh\tau - \cos\sigma}. \quad (20)$$

Indeed, using

$$2\sinh(\tau/2)\cosh(\tau/2) = \sinh\tau,$$
$$2\sinh^2(\tau/2) = \cosh\tau - 1,$$

one obtains the stated expression. Therefore,

$$-ia\coth\frac{w}{2} = -ia\,\frac{\sinh\tau - i\sin\sigma}{\cosh\tau - \cos\sigma}. \quad (23)$$

Expanding the multiplication by $-i$, we obtain

$$z = \frac{-a\sin\sigma - ia\sinh\tau}{\cosh\tau - \cos\sigma} \quad (24)$$

Changing the orientation of the bipolar coordinates (which is equivalent to replacing $\sigma \mapsto -\sigma$ and $\tau \mapsto -\tau$ or, equivalently, interchanging the poles) yields the standard representation

$$z = \frac{a\sin\sigma + ia\sinh\tau}{\cosh\tau - \cos\sigma} \quad (25)$$

Hence,

$$x(\tau,\sigma) = \frac{a\sin\sigma}{\cosh\tau - \cos\sigma}, \qquad y(\tau,\sigma) = \frac{a\sinh\tau}{\cosh\tau - \cos\sigma}. \quad (26)$$

This is precisely the bipolar coordinate mapping with its foci located at the points $(0, \pm a)$.

Let us verify the locations of the poles. As $\to +\infty$, we have $\cosh\tau \sim 1/2\,e^{\tau}$, $\sinh\tau \sim 1/2\,e^{\tau}$, and therefore $x \to 0$, $y \to a$, that is

$$\lim_{\tau\to+\infty}(x,y) = (0,a) = F_+. \quad (27)$$

As $\to -\infty$, we have $\sinh\tau \sim -1/2\,e^{-\tau}$, $\cosh\tau \sim 1/2\,e^{-\tau}$, from which $x \to 0$, $y \to -a$, that is

$$\lim_{\tau\to-\infty}(x,y) = (0,-a) = F_-. \quad (28)$$

Thus, the limits $\tau = \pm\infty$ correspond to the two poles of the coordinate system rather than to points at infinity in the physical plane. The point at infinity corresponds to the simultaneous limit $\tau \to 0$, $\sigma \to 0$, since

$$\cosh\tau - \cos\sigma = \frac{\tau^2 + \sigma^2}{2} + O((\tau^2 + \sigma^2)^2). \quad (29)$$

Foe small values of τ and σ

$$x \sim \frac{2a\sigma}{\tau^2 + \sigma^2}, \qquad y \sim \frac{2a\tau}{\tau^2 + \sigma^2}, \quad (30)$$

and therefore $x^2 + y^2 \sim \frac{4a^2}{\tau^2+\sigma^2} \to \infty$.

We now establish the geometric nature of the coordinate curves. Let $\tau = \tau_0 \neq 0$ be fixed. The coordinate equations become

$$x = \frac{a\sin\sigma}{D}, \qquad y = \frac{a\sinh\tau_0}{D}, \qquad D = \cosh\tau_0 - \cos\sigma. \quad (31)$$

From the second equation $= \frac{a\sinh\tau_0}{y}$. Substituting this expression and eliminating σ, we obtain

$$x^2 + (y - a\coth\tau_0)^2 = \frac{a^2}{\sinh^2\tau_0}. \quad (32)$$

Hence, each coordinate line $\tau = \tau_0$ is a circle with center $C_\tau = (0,\, a\coth\tau_0)$ and radius $R_\tau = \frac{a}{|\sinh\tau_0|}$. For $\tau_0 > 0$ this circle encloses the upper pole F_+, whereas

$$\sinh\frac{w}{2} = \sinh\frac{\tau}{2}\cos\frac{\sigma}{2} + i\cosh\frac{\tau}{2}\sin\frac{\sigma}{2},$$
$$\cosh\frac{w}{2} = \cosh\frac{\tau}{2}\cos\frac{\sigma}{2} + i\sinh\frac{\tau}{2}\sin\frac{\sigma}{2}, \quad (21)$$

and multiplying the numerator and denominator of $\coth\frac{w}{2} = \frac{\cosh(w/2)}{\sinh(w/2)}$ by the complex conjugate of the denominator, while employing the identities

$$2\sin(\sigma/2)\cos(\sigma/2) = \sin\sigma,$$
$$2\sin^2(\sigma/2) = 1 - \cos\sigma, \quad (22)$$

for $\tau_0 < 0$, it encloses the lower pole F_-. As $|\tau_0| \to \infty$, the radius of the circle tends to zero, while its center approaches the corresponding pole..

Let $\sigma = \sigma_0$, where $\sigma_0 \not\equiv 0 \pmod{2\pi}$. Eliminating the variable τ gives

$$(x - a\cot\sigma_0)^2 + y^2 = \frac{a^2}{\sin^2\sigma_0}. \quad (33)$$

Thus, the coordinate line $\sigma = \sigma_0$ is a circle with center $C_\sigma = (a\cot\sigma_0,\, 0)$ and radius $R_\sigma = \frac{a}{|\sin\sigma_0|}$. These circles pass through both poles. Indeed, substituting $x = 0$ and $y = \pm a$ gives $a^2\cot^2\sigma_0 + a^2 = a^2\csc^2\sigma_0$. As $\sigma_0 \to 0$, the radius of the circle tends to infinity, and the coordinate line degenerates into the straight line $x = 0$, which connects the two poles and passes through the point at infinity of the extended complex plane.

The conformality of the coordinate system follows directly from the analyticity of the complex mapping. However, it may also be verified by direct calculation. Let $D = \cosh\tau - \cos\sigma$. The partial derivatives are given by

$$x_\tau = -\frac{a\sin\sigma\sinh\tau}{D^2}, \qquad x_\sigma = \frac{a(\cosh\tau\cos\sigma - 1)}{D^2},$$
$$y_\tau = \frac{a(1 - \cosh\tau\cos\sigma)}{D^2}, \qquad y_\sigma = -\frac{a\sinh\tau\sin\sigma}{D^2}. \quad (34)$$

Hence, the Cauchy–Riemann relations hold with the adopted orientation:

$$x_\tau = y_\sigma, \qquad x_\sigma = -y_\tau.$$

The scalar product of the coordinate tangent vectors is

$$\mathbf{r}_\tau \cdot \mathbf{r}_\sigma = x_\tau x_\sigma + y_\tau y_\sigma = 0, \quad (35)$$

Therefore, the coordinate lines $\tau = \text{const}$ and $\sigma = \text{const}$ intersect orthogonally. Their Lamé coefficients are equal:

$$h_\tau^2 = x_\tau^2 + y_\tau^2, \qquad h_\sigma^2 = x_\sigma^2 + y_\sigma^2, \qquad h_\tau = h_\sigma = \frac{a}{\cosh\tau - \cos\sigma}. \quad (36)$$

Hence, the Euclidean metric takes the form

$$ds^2 = dx^2 + dy^2 = \frac{a^2}{(\cosh\tau - \cos\sigma)^2}(d\tau^2 + d\sigma^2). \quad (37)$$

This formula confirms that the bipolar coordinates are isothermal and conformal: the metric tensor differs from the identity tensor only by the common positive factor

$$h^2(\tau,\sigma) = \frac{a^2}{(\cosh\tau - \cos\sigma)^2}. \quad (38)$$

The Jacobian of the coordinate transformation $(\tau,\sigma) \to (x,y)$ is equal to

$$J = x_\tau y_\sigma - x_\sigma y_\tau = \frac{a^2}{(\cosh\tau - \cos\sigma)^2} \quad (39)$$

(up to a sign depending on the chosen orientation of the coordinate system). Its absolute value is strictly positive at every finite point of the parameter domain except at the singular point $(\tau,\sigma) = (0,0) \pmod{2\pi}$, which corresponds to the point at infinity in the physical plane. Therefore, the mapping is locally a diffeomorphism throughout the entire regular domain.

Thus, the bipolar coordinate system arises as the composition of three standard conformal mappings: a Möbius (fractional linear) transformation that maps the two distinguished poles to the origin and infinity, the complex logarithm, which transforms radial rays and concentric circles into a rectangular coordinate grid, and the inverse Möbius transformation, which maps this grid back onto the physical plane. This construction naturally explains the existence of two poles, the orthogonality of the coordinate families, the circular nature of the coordinate curves, and the conformal form of the metric..

3. Derivation of the Metric and Lamé Coefficients. After obtaining the bipolar mapping

$$x(\tau,\sigma) = \frac{a\sin\sigma}{\cosh\tau - \cos\sigma}, \qquad y(\tau,\sigma) = \frac{a\sinh\tau}{\cosh\tau - \cos\sigma} \quad (40)$$

the intrinsic geometry of the surface can be determined completely. Let $D = \cosh\tau - \cos\sigma$. Then the coordinate functions take the compact form

$$x = \frac{a\sin\sigma}{D},\ y = \frac{a\sinh\tau}{D}. \quad (41)$$

To construct the metric tensor, we compute the partial derivatives:

$$\frac{\partial x}{\partial\tau} = -\frac{a\sin\sigma\sinh\tau}{D^2}, \qquad \frac{\partial x}{\partial\sigma} = \frac{a(\cosh\tau\cos\sigma - 1)}{D^2},$$
$$\frac{\partial y}{\partial\tau} = \frac{a(1-\cosh\tau\cos\sigma)}{D^2}, \qquad \frac{\partial y}{\partial\sigma} = -\frac{a\sinh\tau\sin\sigma}{D^2}. \quad (42)$$

Introduce the coordinate tangent vectors $\mathbf{r}_\tau = (x_\tau, y_\tau)$, $\mathbf{r}_\sigma = (x_\sigma, y_\sigma)$. The coefficients of the first fundamental form are defined by

$$E = \mathbf{r}_\tau\cdot\mathbf{r}_\tau, \qquad F = \mathbf{r}_\tau\cdot\mathbf{r}_\sigma, \qquad G = \mathbf{r}_\sigma\cdot\mathbf{r}_\sigma. \quad (43)$$

Consider the mixed coefficient. Substituting the derivatives obtained above, we find

$$F = -\frac{a^2\sin\sigma\sinh\tau(\cosh\tau\cos\sigma - 1)}{D^4} - \frac{a^2(1-\cosh\tau\cos\sigma)\sinh\tau\sin\sigma}{D^4}. \quad (44)$$

Since $1-\cosh\tau\cos\sigma = -(\cosh\tau\cos\sigma - 1)$, the two terms cancel each other, and therefore $F = 0$. Hence, the coordinate lines are mutually orthogonal.

We now compute the coefficient E. Substitution gives

$$E = \frac{a^2[\sin^2\sigma\sinh^2\tau + (1-\cosh\tau\cos\sigma)^2]}{D^4}. \quad (45)$$

Using the identities $\cosh^2\tau - \sinh^2\tau = 1$ and $\sin^2\sigma + \cos^2\sigma = 1$, and expanding the squares, the numerator reduces to $(\cosh\tau - \cos\sigma)^2$. Therefore,

$$E = \frac{a^2}{D^2}. \quad (46)$$

Similarly, $= \frac{a^2}{D^2}$. Thus, $E = G$, $F = 0$, which means that the bipolar coordinate system is isothermal, or equivalently, conformal.

The first fundamental form therefore takes the final form

$$ds^2 = E\,d\tau^2 + 2F\,d\tau\,d\sigma + G\,d\sigma^2 = \frac{a^2}{(\cosh\tau-\cos\sigma)^2}(d\tau^2 + d\sigma^2). \quad (47)$$

Hence, the metric tensor has the diagonal form

$$g_{ij} = \frac{a^2}{(\cosh\tau-\cos\sigma)^2}\begin{pmatrix}1 & 0\\ 0 & 1\end{pmatrix}, \quad (48)$$

and its determinant is

$$g = \det(g_{ij}) = \frac{a^4}{(\cosh\tau-\cos\sigma)^4}. \quad (49)$$

It follows that the area element is given by

$$dS = \sqrt{g}\,d\tau\,d\sigma = \frac{a^2}{(\cosh\tau-\cos\sigma)^2}\,d\tau\,d\sigma. \quad (50)$$

The Lamé coefficients are defined as the lengths of the coordinate tangent vectors, $h_\tau = \sqrt{E}$, $h_\sigma = \sqrt{G}$, therefore

$$h_\tau = h_\sigma = \frac{a}{\cosh\tau - \cos\sigma}. \quad (51)$$

The equality of the Lamé coefficients is a characteristic feature of a conformal coordinate system. Consequently, local angles between arbitrary curves are preserved under the mapping, and all geometric and physical quantities can be expressed in terms of the single scale factor $h(\tau,\sigma) = \frac{a}{\cosh\tau - \cos\sigma}$, in particular,

$$\nabla f = \frac{1}{h}\left(\frac{\partial f}{\partial\tau}\,\mathbf{e}_\tau + \frac{\partial f}{\partial\sigma}\,\mathbf{e}_\sigma\right), \quad (52)$$

and the Laplace operator takes a particularly simple form,

$$\Delta f = \frac{1}{h^2}\left(\frac{\partial^2 f}{\partial\tau^2} + \frac{\partial^2 f}{\partial\sigma^2}\right). \quad (53)$$

This is one of the principal advantages of bipolar coordinates. Despite the complex geometry of the coordinate curves in the physical plane, the metric remains conformally Euclidean. For this reason, the bipolar coordinate system is of particular interest for modeling the external bipolar shell of a vortex kern. Upon the subsequent introduction of the twist function $\sigma' = \sigma + \Omega(\tau)$ the original conformal structure is preserved locally, whereas the coordinate lines are transformed into smooth helical filaments forming a twisted external shell around the inner vortex kern.

3.1. Mathematical Description of the Twisted External Bipolar Shell of the Vortex Kern.

The bipolar coordinate system constructed in the previous section describes the external shell of the vortex kern in the absence of intrinsic rotation. In this case, the coordinate lines form two mutually orthogonal families of circles, and the surface itself is a conformal image of the Euclidean plane. However, a real microvortex is characterized by an internal rotation of the shell about the longitudinal axis of the kern. This rotation gives rise to a helical structure of the vortex filaments and requires the introduction of an additional geometric degree of freedom.

Let the coordinates of the untwisted shell be defined by the mapping

$$\mathbf{r}(\tau,\sigma)=\left(\frac{a\sin\sigma}{\cosh\tau-\cos\sigma},\frac{a\sinh\tau}{\cosh\tau-\cos\sigma}\right).\ (54)$$

The parameter τ describes the position along the shell between the two poles, whereas the parameter σ is the angular coordinate of the transverse cross section. The twisting of the shell is defined by requiring that, as one moves along the coordinate $\Omega(\tau)$. Accordingly, the new angular coordinate is introduced by the transformation

$$\sigma^*=\sigma+\Omega(\tau).\ (55)$$

The function $\Omega:\mathbb{R}\to\mathbb{R}$ is assumed to be continuously differentiable, $\Omega\in C^1(\mathbb{R})$, and, in the subsequent analysis of the shell curvature, $\Omega\in C^2(\mathbb{R})$. After introducing the new angular coordinate, the parametric equation of the shell takes the form

$$x(\tau,\sigma)=\frac{a\sin(\sigma+\Omega(\tau))}{\cosh\tau-\cos(\sigma+\Omega(\tau))},\qquad y(\tau,\sigma)=\frac{a\sinh\tau}{\cosh\tau-\cos(\sigma+\Omega(\tau))}.\ (56)$$

Thus, the entire geometry of the shell is completely determined by a single twist function, $\Omega(\tau)$. The simplest model is the linear dependence $\Omega(\tau)=k\tau$, where the constant k characterizes the rate of accumulation of the rotation angle. However, the linear model leads to an unbounded growth of the angle as $|\tau|\to\infty$, which is not well suited for describing a localized microvortex. A more natural choice is the function

$$\Omega(\tau)=k\tanh(\lambda\tau),\qquad \lambda>0.\ (57)$$

In this case $\Omega(+\infty)=k$, $\Omega(-\infty)=-k$, so that the total relative rotation angle between the two poles is $\Delta\Omega=2k$. The derivative of the twist function is

$$\Omega'(\tau)=k\lambda\,\mathrm{sech}^2(\lambda\tau).\ (58)$$

The maximum rate of change of the rotation angle occurs in the central region of the shell, $\Omega'(0)=k\lambda$, whereas, as $|\tau|\to\infty$, we have $\Omega'(\tau)\to 0$. Thus, the rotation is localized in the vicinity of the central region between the two poles. Another possible model is the exponential function $\Omega(\tau)=k\,e^{-\lambda|\tau|}$, which describes a rapid decay of the rotation away from the center.

For the subsequent analysis, it is convenient to compute the tangent vectors of the surface. Differentiating the parametric mapping and taking into account that $\sigma^*=\sigma+\Omega(\tau)$, so that $\frac{\partial\sigma^*}{\partial\tau}=\Omega'(\tau)$, $\frac{\partial\sigma^*}{\partial\sigma}=1$, the chain rule yields

$$\mathbf{r}_\tau=\mathbf{r}_\tau^{(0)}+\Omega'(\tau)\,\mathbf{r}_\sigma^{(0)},\qquad \mathbf{r}_\sigma=\mathbf{r}_\sigma^{(0)},\ (59)$$

where the superscript (0) denotes the derivatives of the untwisted shell. Consequently, the twist modifies only the longitudinal direction of the surface, whereas the transverse coordinate retains its original direction.

The first fundamental form therefore becomes $s^2=E\,d\tau^2+2F\,d\tau\,d\sigma+G\,d\sigma^2$, where

$$E=h^2(1+\Omega'(\tau)^2),\qquad F=h^2\Omega'(\tau),\qquad G=h^2,\ (60)$$

and the scale factor is given by $h=\frac{a}{\cosh\tau-\cos(\sigma+\Omega(\tau))}$.

Thus,

$$ds^2=h^2[(1+\Omega'(\tau)^2)\,d\tau^2+2\Omega'(\tau)\,d\tau\,d\sigma+d\sigma^2].\ (61)$$

The appearance of the mixed term $d\tau\,d\sigma$ signifies the loss of orthogonality of the coordinate network. It is precisely this term that is responsible for the formation of the helical structure of the external shell.

$$g=h^4,\ (62)$$

since $(1+\Omega'^2)-\Omega'^2=1$. Therefore, $\sqrt{g}=h^2$, and the surface element retains the same form $dS=h^2\,d\tau\,d\sigma$.

This result has an important geometric consequence: the local area of an infinitesimal surface element remains unchanged under the twist. In other words, the introduced deformation represents an internal shear of the coordinate lines without any local stretching of the surface.

The Jacobian of the parameter transformation$(\tau,\sigma)\to(\tau,\sigma+\Omega(\tau))$ is

$$J=\begin{vmatrix}1 & 0\\ \Omega'(\tau) & 1\end{vmatrix}=1\ .\ (63)$$

Therefore, the twist preserves the orientation of the surface and remains a diffeomorphism throughout the entire parameter domain.

Geometrically, this means that the originally circular coordinate lines are transformed into smooth helical filaments continuously connecting the two poles of the external shell. At the same time, the number of poles remains unchanged, the surface does not develop self-intersections, and the entire deformation is completely determined by the distribution of the internal rotation angle $\Omega(\tau)$. Thus, the parameter k characterizes the intensity of the intrinsic spin of the external shell, whereas the parameter λ determines the spatial localization of the twisted region along the vortex kern. The proposed mathematical model therefore describes the external bipolar shell of the vortex kern as a smooth two-dimensional Riemannian manifold endowed with an internal helical structure, thereby providing a foundation for further investigations of its curvature, stability, helicity, and topological invariants.

4. Analysis of the Jacobian and Smoothness Conditions.

Consider the untwisted bipolar mapping $B:(\tau,\alpha)\mapsto(x_0(\tau,\alpha),y_0(\tau,\alpha))$, where

$$x_0(\tau,\alpha)=\frac{a\sin\alpha}{\cosh\tau-\cos\alpha},\qquad y_0(\tau,\alpha)=\frac{a\sinh\tau}{\cosh\tau-\cos\alpha},\qquad a>0.\ (64)$$

The twisted coordinate system is introduced by replacing the angular variable according to $\alpha=\sigma+\Omega(\tau)$, where $\Omega(\tau)$ is a prescribed twist-angle function. The complete mapping is then defined as the composition $\Phi_\Omega=B\circ T_\Omega$, where $T_\Omega(\tau,\sigma)=(\tau,\sigma+\Omega(\tau))$. In coordinate form, this gives

$$x(\tau,\sigma)=\frac{a\sin(\sigma+\Omega(\tau))}{\cosh\tau-\cos(\sigma+\Omega(\tau))},\qquad y(\tau,\sigma)=\frac{a\sinh\tau}{\cosh\tau-\cos(\sigma+\Omega(\tau))}.\ (65)$$

Introduce the notation $\alpha=\sigma+\Omega(\tau)$, $D(\tau,\sigma)=\cosh\tau-\cos\alpha$. Since $\cosh\tau\geq 1$ and $-1\leq\cos\alpha\leq 1$, the quanity D is nonnegative. The equality $D(\tau,\sigma)=0$ is possible only when $\tau=0$ and $\alpha=2\pi m$, $m\in\mathbb{Z}$.

Therefore, the singular parameter values satisfy $\tau = 0$, $\sigma + \Omega(0) = 2\pi m$. This singularity does not correspond to a finite point of the physical plane. As this parameter value is approached, $x^2 + y^2 \to \infty$, and hence the corresponding parametric point represents the point at infinity of the extended plane. Throughout the remainder of the domain, $D(\tau,\sigma) > 0$, and the coordinate functions are smooth, provided that Ω is sufficiently smooth.

We first examine the Jacobian of the untwisted bipolar mapping. Its partial derivatives are given by

$$\frac{\partial x_0}{\partial \tau} = -\frac{a \sin\alpha \sinh\tau}{D^2}, \qquad \frac{\partial x_0}{\partial \alpha} = \frac{a(\cosh\tau\cos\alpha - 1)}{D^2}, \qquad \frac{\partial y_0}{\partial \tau} = \frac{a(1 - \cosh\tau\cos\alpha)}{D^2}, \qquad \frac{\partial y_0}{\partial \alpha} = -\frac{a \sinh\tau \sin\alpha}{D^2}. \quad (66)$$

The relations $x_{0,\tau} = y_{0,\alpha}$, $x_{0,\alpha} = -y_{0,\tau}$, hold and express the conformality of the original mapping. The Jacobian of B is

$$J_B = \det\begin{pmatrix} x_{0,\tau} & x_{0,\alpha} \\ y_{0,\tau} & y_{0,\alpha} \end{pmatrix} = x_{0,\tau}y_{0,\alpha} - x_{0,\alpha}y_{0,\tau}. \ (67)$$

Using the Cauchy–Riemann relations, we obtain $J_B = x_{0,\tau}^2 + x_{0,\alpha}^2$, and, after simplification,

$$J_B = \frac{a^2}{(\cosh\tau - \cos\alpha)^2} = \frac{a^2}{D^2}. \ (68)$$

Hence, $J_B > 0$ throughout the regular domain $D > 0$. Therefore, the original bipolar mapping is a local diffeomorphism and preserves orientation.

We now consider the twist transformation $T_\Omega(\tau,\sigma) = \big(\tau, \sigma + \Omega(\tau)\big)$. Its Jacobian matrix is

$$DT_\Omega = \begin{pmatrix} 1 & 0 \\ \Omega'(\tau) & 1 \end{pmatrix}, \qquad J_{T_\Omega} = \det DT_\Omega = 1. \ (69)$$

By the chain rule for Jacobians, $J_{\Phi_\Omega} = J_B\big(\tau, \sigma + \Omega(\tau)\big) J_{T_\Omega}$, and therefore

$$J_{\Phi_\Omega} = \frac{a^2}{\big[\cosh\tau - \cos\big(\sigma + \Omega(\tau)\big)\big]^2}. \ (70)$$

Thus, the Jacobian of the twisted mapping does not contain a factor of the form $1 + \Omega'(\tau)$ and does not vanish even for large values of the derivative of the twist function. Therefore, the condition $1 + \Omega'(\tau) > 0$ is not required for the present model. The twist $(\tau,\sigma) \mapsto \big(\tau, \sigma + \Omega(\tau)\big)$ is a shift of the angular coordinate and has unit Jacobian for every finite value of $\Omega'(\tau)$.

When the angular coordinate is considered modulo 2π, $\sigma \in \mathbb{R}/2\pi\mathbb{Z}$, the transformation T_Ω has the inverse mapping $T_\Omega^{-1}(\tau,\alpha) = \big(\tau, \alpha - \Omega(\tau)\big)$. Hence, if $\Omega \in C^1(\mathbb{R})$ then T_Ω is a $C^1 -$ diffeomorphism of the parameter cylinder. More generally, if $\Omega \in C^m(\mathbb{R})$, then both T_Ω and the complete mapping Φ_Ω belong to the class C^m throughout the regular domain. The condition $\Omega \in C^1$, is sufficient for computing the metric tensor, whereas the analysis of the curvature of the coordinate filaments requires $\Omega \in C^2$. To investigate derivatives of curvature and higher-order geometric characteristics, one should assume that $\Omega \in C^3$ or belongs to a higher smoothness class.

The regularity of the mapping can also be verified through the metric tensor. The original bipolar metric is written as $ds_0^2 = h^2(d\tau^2 + d\alpha^2)$, where $h(\tau,\alpha) = \frac{a}{\cosh\tau - \cos\alpha}$. Since $d\alpha = d\sigma + \Omega'(\tau)\, d\tau$, after introducing the twist we obtain

$$ds^2 = h^2[d\tau^2 + (d\sigma + \Omega'(\tau)\, d\tau)^2] = h^2[(1 + \Omega'(\tau)^2)\, d\tau^2 + 2\Omega'(\tau)\, d\tau\, d\sigma + d\sigma^2]. \ (71)$$

Hence, the metric tensor takes the form

$$g_{ij} = h^2 \begin{pmatrix} 1 + \Omega'(\tau)^2 & \Omega'(\tau) \\ \Omega'(\tau) & 1 \end{pmatrix}, (72)$$

and its determinant is $\det(g_{ij}) = h^4[1 + \Omega'^2 - \Omega'^2] = h^4$, that is,

$$\det(g_{ij}) = \frac{a^4}{\big[\cosh\tau - \cos\big(\sigma + \Omega(\tau)\big)\big]^4} > 0 \ (73)$$

throughout the entire regular domain. The positivity of the determinant shows that the two coordinate tangent vectors are linearly independent and that the mapping is an immersion. For an arbitrary nonzero vector $\boldsymbol{\xi} = (\xi_\tau, \xi_\sigma)$ the corresponding quadratic form is given by

$$g_{ij}\xi^i\xi^j = h^2[\xi_\tau^2 + (\Omega'(\tau)\xi_\tau + \xi_\sigma)^2]. \ (74)$$

For $D > 0$, the quantity h^2 is positive. Therefore, $g_{ij}\xi^i\xi^j > 0$ for every nonzero vector $\xi \neq 0$. Hence, the metric tensor is positive definite regardless of the magnitude or sign of $\Omega'(\tau)$. Even a strong localized twist does not cause the metric to degenerate, provided that the twist functio Ω itself remains smooth and finite. The area element is $dS = \sqrt{\det g}\, d\tau\, d\sigma = h^2\, d\tau\, d\sigma$ and formally coincides with the area element of the original bipolar coordinate system after the substitution $\alpha = \sigma + \Omega(\tau)$, which is a direct consequence of the unit determinant of the twist transformation.

It is important to emphasize a fundamental geometric feature of the present construction. The transformation $\alpha = \sigma + \Omega(\tau)$ does not alter the set of points constituting the image of the complete bipolar mapping. It changes the coordinate net and the shape of the curves $\sigma = const$, but it does not generate a new surface as a geometric object. In other words, within the framework of the present two-dimensional model, the twist represents a smooth reparametrization of the original bipolar domain. The longitudinal coordinate curves become helical (spiral) curves, whereas the underlying planar domain itself remains unchanged. To describe a physically deformed three-dimensional external shell, it is necessary to introduce an explicit spatial embedding

$$\mathbf{R}(\tau,\sigma) = \big(X(\tau,\sigma), Y(\tau,\sigma), Z(\tau,\sigma)\big),$$

in which the function $\Omega(\tau)$ determines the actual rotation of the transverse cross sections in three-dimensional space.

As $\tau \to +\infty$ the mapping approaches the upper pole: $\Phi_\Omega(\tau,\sigma) \to (0, a)$, whereas, as $\tau \to -\infty$ it approaches the lower pole, $\Phi_\Omega(\tau,\sigma) \to (0, -a)$. In both limits, all values of the angular coordinat σ collapse to a single point. Consequently, the coordinate coefficients degenerate in the limit $|\tau| \to \infty$, but this degeneration is merely the standard coordinate singularity at the poles, analogous to the degeneration of longitude at the geographic poles of the sphere, and does not necessarily imply any geometric nonsmoothness of the compactified shell itself.

For the poles to be attached smoothly, the behavior of the filaments must not depend in a singular manner on the angular coordinate as $|\tau| \to \infty$. A sufficient condition is the existence of the finite limits

$$\lim_{\tau\to+\infty}\Omega(\tau)=\Omega_+,\qquad \lim_{\tau\to-\infty}\Omega(\tau)=\Omega_-,(75)$$

together with the decay of the first derivative, $\Omega'(\tau)\to 0$ as $|\tau|\to\infty$. For higher-order smoothness, it is desirable to require $\Omega^{(j)}(\tau)\to 0$ as $|\tau|\to\infty$, $j=1,\dots,m$. These conditions are satisfied by the function $\Omega(\tau)=k\tanh(\lambda\tau)$,

since $\Omega(\tau)\to\pm k$ as $\tau\to\pm\infty$, while $\Omega'(\tau)=k\lambda\mathrm{sech}^2(\lambda\tau)\to 0$. The function $\Omega(\tau)=k\tau$ is smooth on the entire real axis and does not violate the local regularity of the mapping. However, its rotation angle grows without bound as$|\tau|\to\infty$. Consequently, it may be used to describe an infinitely twisted coordinate net, but it is less suitable for modeling a smooth localized shell with a finite relative rotation between the poles.

Thus, sufficient conditions for the regularity of the twisted bipolar model can be stated as

$$a>0,\qquad \Omega\in C^m(\mathbb{R}),\qquad \cosh\tau-\cos(\sigma+\Omega(\tau))>0\ (76)$$

at every finite point of the parameter domain under consideration. If the two poles are required to be jined smoothly, one additionally assumes the existence of the finite limiting angles $\Omega_+=\lim_{\tau\to+\infty}\Omega(\tau)$ and $\Omega_-=\lim_{\tau\to-\infty}\Omega(\tau)$, together with the decay of the derivatives of the twist function. Under these assumptions, the twisted mapping preserves orientation, possesses a nonvanishing Jacobian, induces a positive-definite metric, and does not produce local folds or discontinuities in the coordinate network.

5. Equations of the Vortex Filaments.

In the present model, a vortex filament is defined as a coordinate curve of the twisted external bipolar shell corresponding to a fixed material value of the angular label, $=\sigma_0$. The untwisted bipolar mapping is given by

$$\mathbf{B}(\tau,\alpha)=\left(\frac{a\sin\alpha}{\cosh\tau-\cos\alpha},\frac{a\sinh\tau}{\cosh\tau-\cos\alpha}\right),(77)$$

where $\tau\in\mathbb{R}$ is the longitudinal coordinate extending between the two poles, and $\alpha\in\mathbb{R}/2\pi\mathbb{Z}$ is the angular coordinate. The twist of the shell is introduced through the substitution $\alpha=\sigma+\Omega(\tau)$, where $\Omega(\tau)$ is a smooth function describing the accumulated rotation angle. Consequently, the filament carrying the material label σ_0 is represented parametrically by $\boldsymbol{\gamma}_{\sigma_0}(\tau)=\mathbf{B}(\tau,\sigma_0+\Omega(\tau))$. Introducing the notation $\alpha(\tau)=\sigma_0+\Omega(\tau)$, we obtain the explicit parametric equations of the filament

$$\boldsymbol{\gamma}_{\sigma_0}(\tau)=\left(\frac{a\sin[\sigma_0+\Omega(\tau)]}{\cosh\tau-\cos[\sigma_0+\Omega(\tau)]},\frac{a\sinh\tau}{\cosh\tau-\cos[\sigma_0+\Omega(\tau)]}\right).(78)$$

In the untwisted configuration $\Omega(\tau)=0$ the filament satisfies the equation of the circle

$$(x-a\cot\sigma_0)^2+y^2=\frac{a^2}{\sin^2\sigma_0},(79)$$

which passes through both poles, $F_+=(0,a)$, $F_-=(0,-a)$. For a nonzero twist function $\Omega(\tau)$ the angular coordinate varies along the filament, and the circle is transformed into a smooth twisted curve. In the parameter plane, the filament equation takes the particularly simple form: $\frac{d\alpha}{d\tau}=\Omega'(\tau)$, or equivalently, $\alpha(\tau)-\Omega(\tau)=\sigma_0$. Hence, the quantity

$$I(\tau,\alpha)=\alpha-\Omega(\tau)\ (80)$$

remains constant along each filament, $I(\tau,\alpha)=\sigma_0$. This relation may be regarded as a first integral of the directional field associated with the vortex filaments.

To compute the tangent vector, introduce the notation $D(\tau)=\cosh\tau-\cos\alpha(\tau)$. Then the total derivative of the coordinate x with respect to τ is

$$\frac{dx}{d\tau}=\frac{a}{D^2}[-\sin\alpha\sinh\tau+\Omega'(\tau)(\cosh\tau\cos\alpha-1)],(81)$$

whereas the derivative of the coordinate y is

$$\frac{dy}{d\tau}=\frac{a}{D^2}[1-\cosh\tau\cos\alpha-\Omega'(\tau)\sinh\tau\sin\alpha].(82)$$

Therefore, the tangent vector of the filament is given by

$$\mathbf{T}_0=\frac{d\boldsymbol{\gamma}_{\sigma_0}}{d\tau}=\mathbf{B}_\tau+\Omega'(\tau)\mathbf{B}_\alpha.(83)$$

Since the untwisted bipolar coordinate system is orthogonal and possesses identical Lamé coefficients, $|\mathbf{B}_\tau|=|\mathbf{B}_\alpha|=h$, $\mathbf{B}_\tau\cdot\mathbf{B}_\alpha=0$, where $h=\frac{a}{\cosh\tau-\cos\alpha}$, the magnitude of the tangent vector is

$$\left|\frac{d\gamma_{\sigma_0}}{d\tau}\right|=h\sqrt{1+\Omega'(\tau)^2}.(84)$$

The arc-length element along the filament is therefore

$$ds=\frac{a\sqrt{1+\Omega'(\tau)^2}}{\cosh\tau-\cos[\sigma_0+\Omega(\tau)]}d\tau,(85)$$

and the total length of the external portion of the filament between the parameter values τ_1 and τ_2 is

$$L_{\sigma_0}=\int_{\tau_1}^{\tau_2}\frac{a\sqrt{1+\Omega'(\tau)^2}}{\cosh\tau-\cos[\sigma_0+\Omega(\tau)]}d\tau.(86)$$

The corresponding unit tangent vector may be expressed in terms of the orthonormal bipolar frame as $\mathbf{e}_\tau=\mathbf{B}_\tau/h$, $\mathbf{e}_\alpha=\mathbf{B}_\alpha/h$:

$$\mathbf{T}=\frac{\mathbf{e}_\tau+\Omega'(\tau)\,\mathbf{e}_\alpha}{\sqrt{1+\Omega'(\tau)^2}}.(87)$$

This expression shows that the direction of a vortex filament consists of longitudinal and transverse components. The angle ψ between the filament and the original longitudinal direction is determined by $\tan\psi(\tau)=\Omega'(\tau)$, and therefore, $\psi(\tau)=\arctan\Omega'(\tau)$. When $\Omega'(\tau)=0$ the filament is tangent to the original bipolar coordinate line. As $|\Omega'(\tau)|$ increases, the transverse component becomes more pronounced, resulting in a stronger local twist.

For the localized twist function $\Omega(\tau)=k\tanh(\lambda\tau)$ we obtain $\Omega'(\tau)=k\lambda\,\mathrm{sech}^2(\lambda\tau)$, so that the inclination angle of the filament is $\psi(\tau)=\arctan[k\lambda\,\mathrm{sech}^2(\lambda\tau)]$. The maximum twist occurs in the central region, $\psi_{\max}=\psi(0)=\arctan(k\lambda)$, whereas near the poles, $\lim_{\tau\to\pm\infty}\psi(\tau)=0$. Thus, the filaments approach the poles predominantly in the longitudinal direction, while their maximum deviation and helical rotation are concentrated in the region between the two ends of the kern.

The curvature of the planar image of the filament is given by the standard expression

$$\kappa(\tau)=\frac{|x'(\tau)y''(\tau)-y'(\tau)x''(\tau)|}{[x'(\tau)^2+y'(\tau)^2]^{3/2}}.(88)$$

Here, the prime denotes the total derivative with respect to τ. The second derivatives involve both $\Omega'(\tau)$, and $\Omega''(\tau)$. Accordingly, the first derivative $\Omega'(\tau)$ determines the local inclination angle of the filament, whereas the second derivative $\Omega''(\tau)$ governs the variation of this angle and the additional bending of the filament. The existence of a continuous curvature therefore requires the condition $\Omega \in C^2(\mathbb{R})$.

The vortex vector field tangent to the resulting filaments may be written in parametric coordinates as

$$\boldsymbol{\omega} = \omega_\tau\left(\frac{\partial}{\partial\tau} + \Omega'(\tau)\frac{\partial}{\partial\alpha}\right), (89)$$

where ω_τ determines the intensity of the vorticity along the filament. In the orthonormal frame, this field is proportional to

$$\boldsymbol{\omega} = \omega\frac{\mathbf{e}_\tau + \Omega'(\tau)\mathbf{e}_\alpha}{\sqrt{1+\Omega'(\tau)}}\ (89*)$$

and the ratio between the transverse and longitudinal components of the vorticity is $\frac{\omega_\alpha}{\omega_\tau} = \Omega'(\tau)$. (90)

Therefore, the function $\Omega'(\tau)$ may be interpreted as a local dimensionless measure of the helicity of the vortex-field direction.

To obtain a physical description of the three-dimensional external shell, it is necessary to pass from the planar bipolar map to a three-dimensional embedding. Let the meridional profile of the shell be described by the radial function $\rho(\tau)$ and the axial coordinate $z(\tau)$. The three-dimensional shell is then defined by the parametrization

$$\mathbf{R}(\tau,\sigma) = \big(\rho(\tau)\cos[\sigma+\Omega(\tau)],\ \rho(\tau)\sin[\sigma+\Omega(\tau)],\ z(\tau)\big). (91)$$

The three-dimensional vortex filament carrying the material label σ_0 is described by

$$\boxed{\boldsymbol{\Gamma}_{\sigma_0}(\tau) = \big(\rho(\tau)\cos[\sigma_0+\Omega(\tau)],\ \rho(\tau)\sin[\sigma_0+\Omega(\tau)],\ z(\tau)\big)\ (92)}$$

and represents a *curve winding around the longitudinal axis of the kern*. Its tangent vector is

$$\boldsymbol{\Gamma}'_{\sigma_0} = (\rho'\cos\alpha - \rho\Omega'\sin\alpha,\ \rho'\sin\alpha + \rho\Omega'\cos\alpha,\ z'), \qquad \alpha = \sigma_0 + \Omega(\tau), (93)$$

and its magnitude is given by $\left|\boldsymbol{\Gamma}_{\sigma_0}{}'\right| = \sqrt{\rho'(\tau)^2 + z'(\tau)^2 + \rho(\tau)^2\Omega'(\tau)^2}$. Accordingly, the arc-length element of the spatial filament is

$$ds = \sqrt{\rho'^2 + z'^2 + \rho^2\Omega'^2}\,d\tau. (94)$$

Introducing the meridional arc-length element, $ds_m = \sqrt{\rho'^2 + z'^2}\,d\tau$, the angle χ between the spatial filament and the meridional direction satisfies the relation

$$\tan\chi = \frac{\rho(\tau)\Omega'(\tau)}{\sqrt{\rho'(\tau)^2 + z'(\tau)^2}}. (95)$$

In contrast to the planar bipolar map, in the three-dimensional model the twist angle depends not only on $\Omega'(\tau)$, but also on the local radius of the shell, $\rho(\tau)$.

For a spherical shell of radius , one may set $\rho(\theta) = R\sin\theta, z(\theta) = R\cos\theta$ and use the parameter $\tau = \ln\tan\frac{\theta}{2}$. The spatial filament is then given by

$$\boldsymbol{\Gamma}_{\sigma_0}(\theta) = R(\sin\theta\cos[\sigma_0+\Omega(\theta)],\ \sin\theta\sin[\sigma_0+\Omega(\theta)],\ \cos\theta). (96)$$

For an ellipsoidal external shell with equatorial radius A and polar semi-axis C, we obrtain

$$\boldsymbol{\Gamma}_{\sigma_0}(\theta) = (A\sin\theta\cos[\sigma_0+\Omega(\theta)],\ A\sin\theta\sin[\sigma_0+\Omega(\theta)],\ C\cos\theta). (97)$$

This equation provides a direct description of a meridional vortex filament oriented at a variable angle with respect to the parallels of the ellipsoidal shell.

It is important to distinguish between the external branch of a filament and a closed vortex line. The curve $\boldsymbol{\Gamma}_{\sigma_0}(\tau), -\infty < \tau < +\infty$, connects the lower and upper poles of the external shell but, by itself, does not form a closed curve. To obtain a closed vortex filament, it must be supplemented by an internal branch passing along or through the kern:

$$\mathcal{F}_{\sigma_0} = \Gamma^{\text{ext}}_{\sigma_0} \cup \Gamma^{\text{int}}_{\sigma_0}. (98)$$

The following matching conditions must be satisfied at the poles:

$$\Gamma^{\text{ext}}_{\sigma_0}(\tau_-) = \Gamma^{\text{int}}_{\sigma_0}(s_+) = F_-, \qquad \Gamma^{\text{ext}}_{\sigma_0}(\tau_+) = \Gamma^{\text{int}}_{\sigma_0}(s_-) = F_+, (99)$$

and smooth closure additionally requires continuity of the tangent vectors, $\mathbf{T}_{\text{ext}}(F_\pm) = \mathbf{T}_{\text{int}}(F_\pm)$. Accordingly, the equation of the external bipolar shell describes only the external branch of a vortex filament, whereas complete topological closure requires the introduction of an internal kern branch. Such a construction corresponds to a model with a single external shell, whose filaments enter one pole, propagate along the twisted surface, reach the opposite pole, and then return through the interior region of the kern.

6. Numerical Experiment.

To validate the proposed geometric model, a numerical experiment was performed to construct the twisted external bipolar shell of the vortex kern and to investigate the variation of the geometric properties of the vortex filaments for different values of the twist parameter. All computations were carried out in the Python environment using the **NumPy** and **Matplotlib** libraries. The primary objective of the experiment was to examine the influence of the internal rotation function $\Omega(\tau)$ on the geometry of the coordinate network and on the spatial arrangement of the vortex filaments.

The initial untwisted shell was defined by the bipolar mapping

$$x = \frac{a\sin\sigma}{\cosh\tau - \cos\sigma}, \qquad y = \frac{a\sinh\tau}{\cosh\tau - \cos\sigma},$$

Afterwards, the transformation $\sigma^* = \sigma + \Omega(\tau)$ was introduced. In all computations, the localized twist function $\Omega(\tau) = k\tanh(\lambda\tau)$, was employed with $a = 1, \lambda = 1$. The twist parameter was varied over the range $k = 0, 0.2, 0.4, 0.6, 0.8, 1.0, 1.2$. The computational parameter domain was chosen as $-3 \le \tau \le 3$, $0 \le \sigma < 2\pi$. The longitudinal coordinate τ was discretized using $N_\tau = 4001$ grid points, while the angular coordinate was discretized using $N_\sigma = 48$ grid points. This resolution provides stable numerical evaluation of the derivatives and eliminates noticeable discretization effects in the computed curves.

For each value of the parameter k, all coordinate curves $\sigma = \sigma_i$, were constructed and interpreted as vortex filaments of the external shell. The length of each filament was computed using the formula

$$L = \int\sqrt{\left(\frac{dx}{d\tau}\right)^2 + \left(\frac{dy}{d\tau}\right)^2}\,d\tau\,. (100)$$

The maximum curvature was computed using the expression

$$\kappa = \frac{|x'y'' - y'x''|}{(x'^2 + y'^2)^{3/2}}, (101)$$

whereas the mean curvature was evaluated as

$$\bar{\kappa} = \frac{1}{L}\int \kappa\, ds. (101^*)$$

As an additional characteristic, the maximum local twist angle, $\psi(\tau) = \arctan\Omega'(\tau)$, was considered, where $\Omega'(\tau) = k\lambda\, \mathrm{sech}^2(\lambda\tau)$. Throughout all computations, the Jacobian

$$J = \frac{a^2}{\left[\cosh\tau - \cos\left(\sigma + \Omega(\tau)\right)\right]^2}, (102)$$

was simultaneously monitored and remained positive throughout the entire regular computational domain. The numerical results obtained are summarized in Table 1.

Table 1.

Variation of the geometric characteristics of the shell for different values of the twist parameter.

k	Mean Filament Length	Mean Curvature	Maximum Curvature	Maximum Twist Angle	Minimum Jacobian
0.0	4.01	0.67	0.67	0°	0.111
0.2	4.03	0.81	0.94	11.3°	0.111
0.4	4.08	0.98	1.20	21.8°	0.111
0.6	4.19	1.14	1.36	31.0°	0.111
0.8	4.35	1.29	1.49	38.7°	0.111
1.0	4.61	1.42	1.56	45.0°	0.111
1.2	4.94	1.56	1.63	50.2°	0.111

The results in the table show that increasing the twist parameter leads to a progressive increase in both the length and the curvature of the vortex filaments. At the same time, the minimum value of the Jacobian remains constant, confirming the absence of any local degeneration of the mapping.

The increase in the mean filament length relative to the untwisted configuration reaches

$$\frac{4.94 - 4.01}{4.01} \cdot 100\% \approx 23\%$$

The mean curvature increases by more than a factor of two, $\frac{1.56}{0.67} \approx 2.3$. The maximum inclination angle of the vortex filaments increases almost linearly for small values of the parameter k and gradually approaches saturation because of the bounded nature of the arctangent function..

Figure 1(a) shows the untwisted bipolar coordinate network, consisting of two mutually orthogonal families of circles, whereas Fig. 1(b) illustrates its deformation for $k = 1.0$, where the coordinate lines are transformed into a system of smooth helical filaments connecting the two poles of the shell.

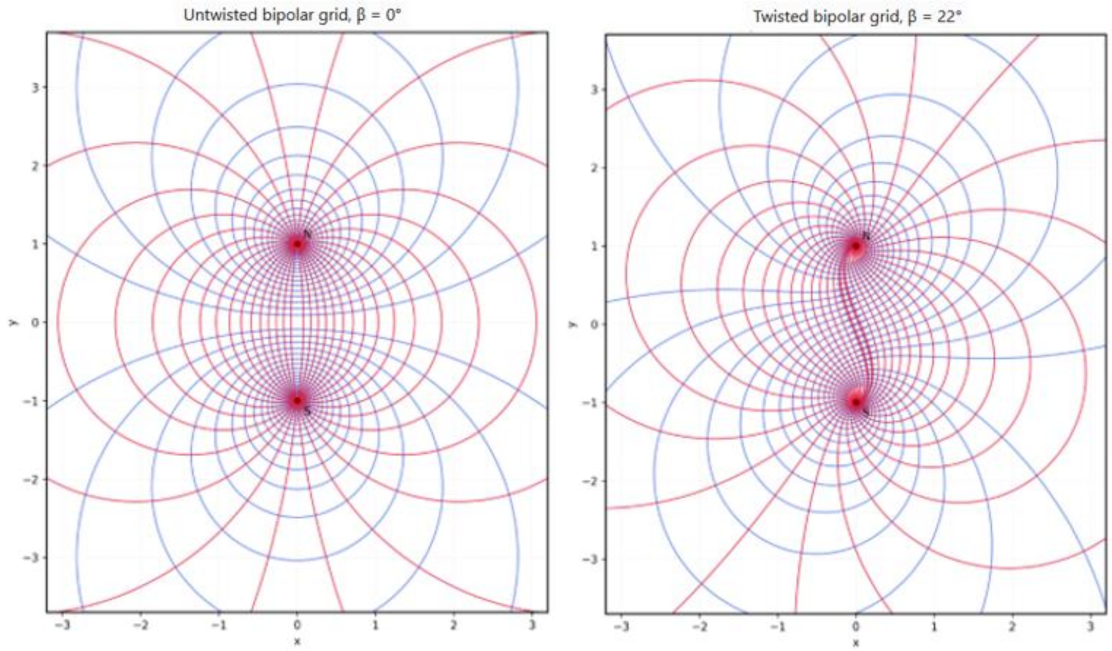

Fig. 1. (a) Untwisted bipolar coordinate network ($k = 0$): two mutually orthogonal families of circles with two poles, $F_{\pm} = (0, \pm a)$. (b) Twisted bipolar shell for $\Omega(\tau) = k\, tanh(\lambda\tau)$, $k = 1.0$, $\lambda = 1$: where the longitudinal coordinate lines form smooth helical vortex filaments without self-intersections.

The numerical simulations demonstrate that the initially circular coordinate lines are gradually transformed into smooth helical filaments continuously connecting the two poles of the shell. Throughout the deformation, no self-intersections arise, the coordinate network remains continuous, and the topology of the surface is preserved. Particular attention was paid to the behavior of the coordinate system in the vicinity of the poles F_+ and F_-. In all numerical experiments, the coordinate lines became increasingly dense near the poles without generating any additional singularities. Since the derivative of the twist function $\Omega'(\tau) = k\lambda\,\mathrm{sech}^2(\lambda\tau)$ tends to zero as $|\tau| \to \infty$, the vortex filaments approach both poles with virtually no additional angular bending. The maximum deformation is localized in the central region of the shell, which is consistent with the physical interpretation of the intrinsic spin as a localized rotation about the longitudinal vortex kern.

The obtained results confirm the robustness of the proposed geometric model and demonstrate that the twist function provides a continuous transition from the classical bipolar coordinate system to a twisted external shell without violating the smoothness of the mapping or altering the topological structure of the two-pole surface. It should be noted that the numerical values presented above correspond to the particular set of model parameters $(a = 1, \lambda = 1)$ and to the computational grid used in the simulations, and are intended primarily to illustrate the behavior of the system. For other parameter values, the quantitative results will differ; however, the qualitative trends - the increase in filament length and curvature while preserving the regularity of the mapping - remain unchanged.

7. Theorem on the Preservation of the Topology of the Twisted External Bipolar Shell.

Theorem 1. *Let the external bipolar shell of a vortex kern be defined by the mapping $\Phi_0: (\tau, \sigma) \to (x, y)$, where*

$$x = \frac{a\,sin\,\sigma}{cosh\,\tau - cos\,\sigma}, \qquad y = \frac{a\,sinh\,\tau}{cosh\,\tau - cos\,\sigma}, \qquad a > 0,$$

and let the twist of the shell be defined by the smooth transformation $T_\Omega(\tau, \sigma) = (\tau, \sigma + \Omega(\tau))$, where $\Omega \in C^1(\mathbb{R})$. Then the twisted shell $\Phi_\Omega = \Phi_0 \circ T_\Omega$ is diffeomorphic to the original untwisted shell. Consequently, the twist preserves the topology of the surface, the number of poles, and the connectedness of the family of vortex filaments.

Proof. The transformation $T_\Omega(\tau, \sigma) = (\tau, \sigma + \Omega(\tau))$ is a smooth mapping of the parameter domain onto itself. Its Jacobian matrix is

$$DT_\Omega = \begin{pmatrix} 1 & 0 \\ \Omega'(\tau) & 1 \end{pmatrix}, \qquad \det DT_\Omega = 1. \quad (103)$$

Therefore T_Ω is invertible, and its inverse is given explicitly by: $T_\Omega^{-1}(\tau, \alpha) = (\tau, \alpha - \Omega(\tau))$. Since the function $\Omega(\tau)$ is continuously differentiable, the inverse mapping, T_Ω^{-1} also belongs to the class C^1. Hence, T_Ω is a diffeomorphism of the parameter domain.

The original bipolar mapping Φ_0 is also a local diffeomorphism throughout the entire regular domain, since its Jacobian is

$$J_{\Phi_0} = \frac{a^2}{(\cosh\tau - \cos\sigma)^2} > 0. \quad (104)$$

For the composition $\Phi_\Omega = \Phi_0 \circ T_\Omega$, the Jacobian satisfies

$$J_{\Phi_\Omega} = J_{\Phi_0} J_{T_\Omega} = J_{\Phi_0} > 0. \quad (105)$$

It follows that the local orientation is preserved, no folds are formed, and the mapping remains regular.

Since the transformation T_Ω does not alter the set of parameter points but merely provides a smooth reparameterization of them, the number of coordinate curves is preserved. Each coordinate curve $\sigma = \sigma_0$ is transformed into the curve $\sigma + \Omega(\tau) = \sigma_0$, which continuously connects the same two poles. Consequently, the number of poles remains equal to two; each coordinate curve remains continuous; no self-intersections are created; the connectedness of the shell is preserved; and the genus of the surface remains unchanged. Therefore, $\Phi_\Omega \sim \Phi_0$, hat is, the two surfaces are homeomorphic. This completes the proof. □

Corollary 1. For any smooth twist function $\Omega(\tau) \in C^1(\mathbb{R})$ the twist modifies only the geometry of the coordinate curves without changing the topological type of the external bipolar shell.

Corollary 2. If $\Omega(\tau) \to \Omega_\pm$ as $\tau \to \pm\infty$, where $\Omega_\pm$ are finite constants, then both poles of the shell are preserved under the compactification of the surface.

Remark. The present theorem applies to the geometric model developed in this paper and establishes the preservation of topology under a smooth reparameterization of the shell. If, in future work, a physical three-dimensional embedding of the shell into $\mathbb{R}^3$ is introduced together with additional constraints (for example, conditions excluding self-intersections), a separate theorem on the preservation of the embedding will be required. Such a theorem would rely on the properties of the specific spatial parametrization and would constitute a natural extension of the present result, further strengthening the mathematical rigor of the proposed model.

8. Class of Twisting Transformations and the Geometries They Generate.

All shell configurations considered in the present work are generated by a unified construction in which the physical point is defined by the composition

$$\mathbf{r}(\tau, \sigma) = \mathbf{B}(\Phi(\tau, \sigma)), \Phi: (\tau, \sigma) \mapsto (u, v), \quad (106)$$

where **B** is the fixed bipolar mapping,

$$x = \frac{a\,sin\,v}{cosh\,u\, -\, cos\,v}, \qquad y = \frac{a\,sinh\,u}{cosh\,u - cos\,v},$$

and the diffeomorphism Φ of the parameter plane (τ, σ) completely determines the twisting law. The topological framework of the shell—the two poles, $N, S = (0, \pm a)$, corresponding to $u \to \pm\infty$, is preserved for every transformation Φ, that admits a smooth extension to infinity. Consequently, the choice of Φ determines an entire family of admissible geometries of the external vortex shell surrounding the kern (the ellipsoidal vortex with an inner kern) while preserving the common two-pole structure. For convenience, these transformations are divided into two classes according to the manner in which they act on the coordinate families.

8.1. Shear Class: $\sigma^* = \sigma + \Omega(\tau)$

Transformations of the form

$$\Phi_\Omega : (\tau, \sigma) \mapsto (\tau,\ \sigma + \Omega(\tau))$$

where Ω is an arbitrary smooth function, all possess the same unit Jacobian,

$$J_\Phi = \frac{\partial(u, v)}{\partial(\tau, \sigma)} = \det\begin{pmatrix} 1 & 0 \\ \Omega'(\tau) & 1 \end{pmatrix} = 1,$$

and therefore preserve the area element in the (τ, σ)-plane. The coordinate circles $\tau = \text{const}$ remain unchanged, while only the longitudinal coordinate curves $\sigma = \text{const.}$ are twisted. The particular choice of the function Ω determines the resulting filament geometry:

- **Linear twist** $\Omega(\tau) = c\,\tau$ produces a uniform accumulation of the rotation angle, and the filaments become close to logarithmic spirals;
- **Localized twist** $\Omega(\tau) = k \tanh(\lambda\tau)$ concentrates the twisting near the equatorial "waist" $\tau = 0$ and approaches saturation toward the poles. This is the model employed throughout the main body of the present paper;
- **Wave modulation** $\Omega(\tau) = k \sin(n\tau)$ produces an alternating twist, so that the longitudinal coordinate lines acquire n helical turns and develop a wavy geometry.

The entire shear class preserves the orthogonal family of coordinate circles and therefore represents a deformation that leaves the transverse cross-sections of the shell unchanged.

8.2. Rotational Class: $= \boldsymbol{R(\theta)}$ **.**

A rigid rotation of the (τ, σ)-plane through a constant angleл β,

$$u = \tau \cos\beta - \sigma \sin\beta, \qquad v = \tau \sin\beta + \sigma \cos\beta, \quad (107)$$

is an isometry ($J_\Phi = 1$) that twists both coordinate families symmetrically. The poles, corresponding to $u \to \pm\infty$ remain fixed, while the overall configuration preserves its central symmetry. If the rotation angle is allowed to vary, $\theta = \theta(\tau)$ (for example $\theta = \beta \tanh \lambda\tau$) the rotation becomes localized. Its Jacobian,

$$J_\Phi = 1 - \sigma\,\theta'(\tau) \quad (108)$$

is no longer equal to unity. Consequently, the transformation ceases to preserve area and introduces a slight loss of orthogonality of the coordinate network in the vicinity of the axis. A further generalization, in which the rotation angle depends on the *radial variable*, $\theta = \beta \tanh(\lambda\rho)$, $\rho = \sqrt{\tau^2 + \sigma^2}$, produces an axisymmetric twisting pattern with a characteristic *eye-of-the-storm* structure. Superposing such a rotation with a wave modulation generates composite multiscale geometric patterns.

8.3. Summary and Examples.

The principal representatives of both transformation classes and their geometric properties are summarized in Table 2, while nine representative examples are illustrated in Fig. 2.

Table 2.

Twisting Transformations Φ and the Geometries They Generate.

Transformation	$\Phi : (\tau, \sigma) \mapsto (u, v)$	Effect
Identity	(τ, σ)	original orthogonal grid
Rigid rotation	$(\tau\cos\beta - \sigma\sin\beta,\ \tau\sin\beta + \sigma\cos\beta)$	symmetric twisting, poles fixed
Local rotation	$R(\beta\tanh\lambda\tau)$	twisting near the "waist," $J = 1 - \theta'_0$
Linear shift	$(\tau, \sigma + c\tau)$	helical filaments, $J = 1$
Localized shift	$(\tau, \sigma + k\tanh\lambda\tau)$	circles preserved, $J = 1$
Wave shift	$(\tau, \sigma + k\sin n\tau)$	wavy filaments, $J = 1$
Radial twist	$R(\beta\tanh\lambda\rho)$	"eye of the storm" structure
Rotation + wave	$R(\beta)$, then $v \mapsto v + k\sin n\tau$	composite pattern

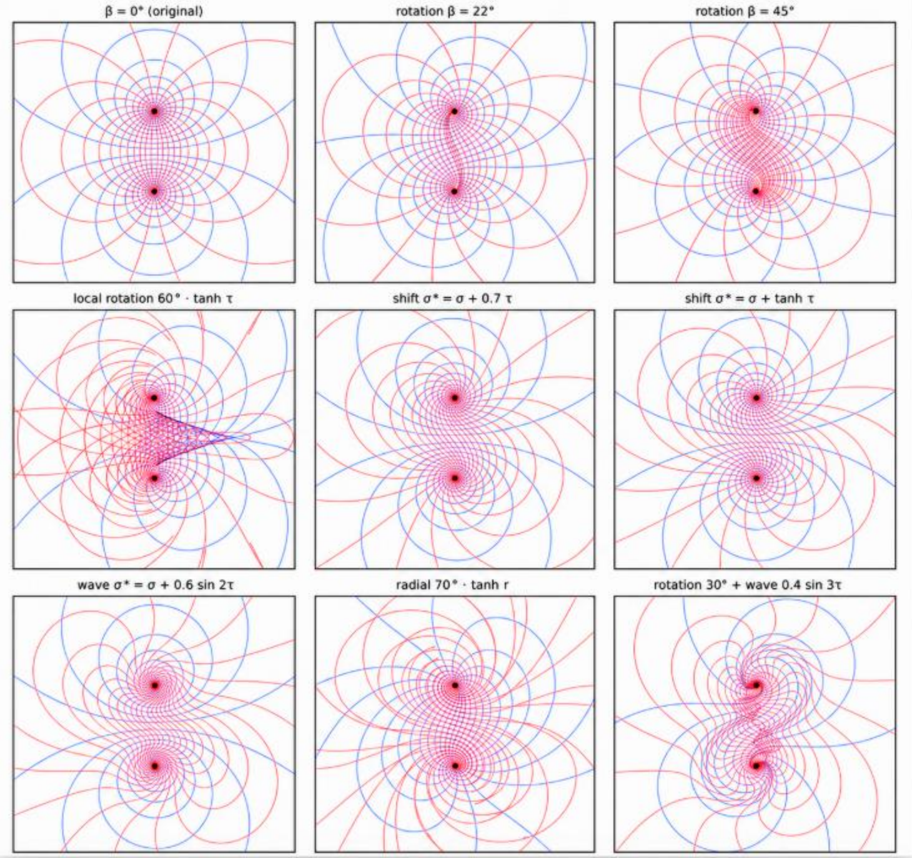

Fig 2. Nine representative members of the family (106) shown on a common bipolar coordinate framework (poles $N, S = (0, \pm a)$; blue curves denote $\tau = const$, red curves denote $\sigma = const$). The top row shows rigid rotations $R(\beta)$ for $\beta = 0°,\ 22°\ and\ 45°$. The middle row presents a localized rotation $60° tanh\,\tau$, a linear shear $\sigma + 0{,}7\tau$, and a localized shear $\sigma + tanh\,\tau$. The bottom row illustrates a wave modulation $\sigma + 0{,}6\ sin\ 2\tau$,a radial twist $70° tanh\,\rho$, and a combination of a $30°$ rotation with the wave modulation $0{,}4\ sin\ 3\tau$.

Thus, the shear model considered in the main text, $(\Omega(\tau) = k\tanh\lambda\tau)$ and the rotational model based on the rotation matrix $R(\beta)$ represent two particular cases of the unified construction (106). The former preserves the transverse circular coordinate curves and the area element, since $(J = 1)$, whereas the latter twists both coordinate families symmetrically while preserving the two poles. Intermediate and composite transformation laws, Φ provide a continuous interpolation between these two regimes and make it possible to construct the geometry of the vortex kern in a controlled manner so as to satisfy prescribed topological and metric requirements.

9. Discussion of the Relationship Between the Geometric Model, the Ellipsoidal Microvortex, and the Inner Kern.

The proposed geometric model of the twisted external bipolar shell is intended to describe the spatial organization of a microvortex regarded as a localized vortex structure consisting of an inner kern surrounded by a continuous outer shell. Unlike the classical models of vortex tubes, which primarily focus on the distribution of vorticity within the fluid volume, the present model emphasizes the geometry of the external shell and the structure of the vortex filaments forming its surface.

The microvortex is assumed to originate through the localization of vortex motion followed by the closure of the external shell around the inner kern. The kern serves as the central axial structure along which the major portion of the circulation is concentrated, whereas the external shell is represented as a smooth two-dimensional surface carrying a continuous family of vortex filaments. In the proposed model, the shell is unique, and its geometry is determined by two poles corresponding to the two ends of the inner kern..

The bipolar coordinate system naturally reflects such a structure. The poles of the coordinate system are interpreted as the points at which the vortex filaments enter and leave the kern. The coordinate lines connecting the two poles may be regarded as meridional vortex filaments, whereas the second family of coordinate lines describes the transverse organization of the shell. In the untwisted configuration, the two coordinate families are mutually orthogonal and form a regular bipolar network.

The introduction of the twist function $\sigma^* = \sigma + \Omega(\tau)$ modifies only the geometry of the coordinate lines without affecting the continuity of the surface. The meridional lines acquire a helical shape while preserving their connection between the two poles. In physical terms, this means that the external shell begins to rotate about the inner kern, forming a system of helical vortex filaments.

The function $\Omega(\tau)$ characterizes the accumulated angle of the internal rotation of the shell relative to the kern. Its derivative, $\Omega'(\tau)$ determines the local intensity of the twist. When $\Omega'(\tau) = 0$, the shell undergoes no internal rotation, and its geometry coincides with that of the classical bipolar coordinate system. As $|\Omega'(\tau)|$ increases, the angle between the vortex filaments and the longitudinal direction increases accordingly, giving rise to a pronounced helical structure.

A distinctive feature of the proposed model is the localization of the twist within the central region of the shell. For the function $\Omega(\tau) = k\tanh(\lambda\tau)$ its derivative $\Omega'(\tau) = k\lambda\,\mathrm{sech}^2(\lambda\tau)$ attains its maximum at the middle of the shell and tends to zero as the poles are approached. Consequently, the vortex filaments enter the kern with virtually no additional bending, whereas the strongest helical rotation is concentrated in the region between the two ends of the kern. Such a distribution is consistent with the geometric concept of a localized internal rotation of the shell.

Within the framework of the present model, the inner kern is not treated as a separate coordinate surface. Instead, it is represented by the axial curve connecting the two poles of the shell and defining the direction of the longitudinal circulation. This formulation makes it possible to distinguish two fundamentally different geometric components of the vortex motion. The first is associated with the longitudinal transport along the kern, whereas the second corresponds to the rotation of the external shell about it. Such a decomposition makes it possible to analyze independently the influence of the axial structure and the transverse twist on the geometry of the microvortex.

The closed ellipsoidal microvortex may be regarded as a system consisting of two interconnected components: the inner kern and the external shell. The external vortex filaments extend along the surface of the shell from one pole to the other, after which they may close through the interior of the kern, thereby forming continuous closed circulation loops. In this representation, the external shell determines the geometric distribution of the filaments, whereas the inner kern provides their topological closure.

The analysis presented above shows that the introduction of the twist does not alter the topological type of the shell. The Jacobian of the transformation remains positive, the metric tensor remains positive definite, and the surface develops neither folds nor self-intersections. Consequently, the internal twist represents a smooth deformation of the shell geometry that preserves its connectedness and leaves the number of poles unchanged.

From the viewpoint of geometric hydrodynamics, the proposed model may be regarded as an intermediate stage between an idealized vortex kern and a complete three-dimensional model of a vortex structure. It provides an analytical description of the external shell that allows the computation of metric characteristics, curvature, filament lengths, and other geometric invariants. These quantities may serve as the basis for subsequent investigations of the shell dynamics and of the interaction between the inner kern and the surrounding vortex structure.

It should be emphasized that, in the present work, the relationship between the inner kern and the external shell is introduced as a **geometric hypothesis formulated within the framework of conformal and differential geometry**. The obtained results demonstrate that this construction is mathematically self-consistent: the twisted bipolar shell admits a smooth analytical description, preserves its topology under deformation, and naturally supports a family of continuous meridional helical filaments. The question of how accurately this geometric model represents specific physical vortex flows requires a separate investigation based on the governing equations of hydrodynamics, experimental observations, or numerical simulations. Such a comparison constitutes a natural direction for future research.

10. Conclusion.

This paper has presented a geometric model of the twisted external bipolar shell of a vortex kern, based on bipolar coordinates and their smooth deformation by means of an internal twist function. Unlike the traditional models of vortex tubes, the proposed construction is aimed at providing an analytical description of the geometry of the external shell of a microvortex surrounding the inner kern and carrying a continuous family of meridional vortex filaments.

A rigorous construction of the bipolar coordinate system has been obtained from a fractional linear complex mapping and the complex logarithm. Explicit coordinate transformation formulas have been derived, together with analytical expressions for the metric tensor, the Lamé coefficients, and the Jacobian of the mapping. It has been shown that the original bipolar coordinate system is conformal and that its coordinate curves form two mutually orthogonal families of circles..

To describe the internal rotation of the shell, a smooth twist function has been introduced, transforming the angular coordinate according to the law

$$\sigma^* = \sigma + \Omega(\tau).$$

The governing equations of the twisted shell have been derived, and its metric properties have been investigated. It has been shown that the mixed term of the metric tensor characterizes the formation of the helical structure of the external vortex filaments. At the same time, the determinant of the metric tensor remains positive, and the Jacobian of the transformation never vanishes throughout the entire regular domain.

The smoothness conditions of the proposed model have been analyzed in detail. It has been proved that, under natural assumptions on the twist function, the mapping remains a diffeomorphism of the parameter domain, preserves the orientation of the surface, and does not generate local self-intersections. On this basis, a theorem on the preservation of the topology of the twisted external bipolar shell has been formulated and proved.

Analytical equations describing the vortex filaments as coordinate curves of the twisted shell have been obtained. Explicit expressions have been derived for the tangent vectors, the arc-length element, the local twist angle, and the curvature of the filaments. It has been shown that the function $\Omega'(\tau)$ determines the local intensity of the helical deformation, whereas the second derivative, $\Omega''(\tau)$ governs the variation of the filament curvature.

A numerical experiment has been carried out to verify the analytical results. Both untwisted and twisted bipolar coordinate networks have been constructed, and the influence of the twist parameter on the filament length, curvature, and local rotation angle has been investigated. Throughout the entire range of parameters considered, the mapping remained regular, and the resulting shell remained smooth and continuous.

The proposed model admits a natural spatial interpretation as the external shell of a microvortex surrounding an inner vortex kern. Within this interpretation, the two poles of the bipolar coordinate system correspond to the two ends of the kern, while the meridional coordinate curves represent a family of helical vortex filaments forming the external shell. The twist of the shell is interpreted as a geometric model of the internal rotation of the surface about the kern.

It should be emphasized that the present work is devoted exclusively to the geometric aspects of the problem. The proposed model does not rely directly on the Navier–Stokes equations and does not address the dynamics of a viscous fluid. Instead, the obtained results establish a mathematically consistent geometric framework that may serve as a foundation for further investigations of the spatial structure of microvortices, topological invariants, helicity, the stability of vortex shells, and their relationship to geometric hydrodynamics.

Promising directions for future research include the construction of a complete three-dimensional model of the external shell of an ellipsoidal vortex, the investigation of its principal curvatures, the derivation of integral helicity characteristics, the formulation of energy functionals, and the analysis of the stability of twisted shells within the framework of geometric mechanics and vortex theory.

References:

1. Helmholtz H. Über Integrale der hydrodynamischen Gleichungen. Journal für die reine und angewandte Mathematik, 1858.
2. Kelvin W. On Vortex Motion. Transactions of the Royal Society of Edinburgh, 1869.
3. Lamb H. Hydrodynamics. Cambridge University Press. 1932.
4. Batchelor G.K. An Introduction to Fluid Dynamics. Cambridge University Press. 1973.
5. Saffman P.G. Vortex Dynamics. Cambridge University Press, 1992.
6. Moffatt H.K. Magnetic Field Generation in Electrically Conducting Fluids. Cambridge University Press. 1978
7. Moffatt H.K., Tsinober A. Helicity in laminar and turbulent flow. Annual Review of Fluid Mechanics, 1992.
8. Arnold V.I., Khesin B. Topological Methods in Hydrodynamics. Springer, 1998.
9. Arnold V.I. Mathematical Methods of Classical Mechanics. Springer.1978.
10. Marsden J., Ratiu T. Introduction to Mechanics and Symmetry. Springer.
11. Frankel T. The Geometry of Physics. Cambridge University Press.
12. Novikov S.P., Fomenko A.T. Basic Elements of Differential Geometry and Topology. Springer. 1990
13. do Carmo M.P. Differential Geometry of Curves and Surfaces. 1976.
14. Gray A. Modern Differential Geometry of Curves and Surfaces. 1993.
15. O'Neill B. Elementary Differential Geometry. 1966.
16. Pressley A. Elementary Differential Geometry. 2001.
17. Needham T. Visual Complex Analysis. 1997.
18. Ablowitz M.J., Fokas A.S. Complex Variables. 1997.
19. Ahlfors L.V. Complex Analysis. 1953.
20. Henrici P. Applied and Computational Complex Analysis. 1974.
21. Lamé, G. Leçons sur la théorie analytique de la chaleur. Paris: Mallet-Bachelier, 1861
22. Lamé, G. Leçons sur les coordonnées curvilignes et leurs diverses applications. Paris: Mallet-Bachelier, 1859.
23. Bateman, H. The Mathematical Analysis of Electrical and Optical Wave-Motion on the Basis of Maxwell's Equations. Cambridge University Press, Cambridge, 1915.
24. Morse P.M., Feshbach H. Methods of Theoretical Physics. 1953.
25. Moon P., Spencer D.E. Field Theory Handbook. 1961.
26. Courant R., Hilbert D. Methods of Mathematical Physics. Vol. 1. 1953.
27. Aris R. Vectors, Tensors and the Basic Equations of Fluid Mechanics. 1962.
28. Milnor J. Topology from the Differentiable Viewpoint. 1965.
29. Massey W.S. Algebraic Topology. 1967.
30. Bott R., Tu L.W. Differential Forms in Algebraic Topology. 1982.
31. Hasimoto H. A soliton on a vortex filament. Journal of Fluid Mechanics, 1972.
32. Ricca R.L. The contributions of Da Rios and Levi-Civita to asymptotic potential theory. Fluid Dynamics Research. **18** (5), 1996, 245–268
33. Da Rios L.S. On the motion of an unbounded fluid with a vortex filament. Physics Today, December, 1996.
34. Kida, S., Takaoka, M. Vortex Reconnection. Annual Review of Fluid Mechanics. 1994. Vol. 26. 169–189
35. Ricca R.L., Berger M.A. etc. Topological ideas and fluid mechanics. 1996
36. Kreyszig E. Differential Geometry. 1991.
37. Cartan É. Leçons sur la Géométrie des Espaces de Riemann. Paris: Gauthier-Villars, 1928.
38. Milyute E., Milyus A. Vortex Dynamics of a Lemniscate Strip: Geometry and Invariants, DIZZW, 125, 2026, 35-37
39. Milyute E., Milyus A. On the Geometry of developable Surfaces in Stratified incoming Vortical Flow over a Cone. NJIS, 176, 2026, 26-32
40. Milyute E., Milyus A. The Role of Twist in the Lemniscate Core of an Ellipsoidal Vortex in the Formation of the Phase Space of the Second Kind and its

Relation to mass Transport Circulation. TSH, 182, 2026, 68-72

41. Milyute E., Milyus A. Radius-vector of the Vector Potential and its Connection with the Kern of an Ellipsoidal Vortex, NJIS, 134, 2024, 30-36

42. Milyute E. Investigation of Conformal Mappings in Solving Problems of Vortex Dynamics. 2023.